Properties of Amorphous Calcium Carbonate and the Template Action of Vaterite Spheres

Qiang Shen,*,†,‡ Hao Wei,† Yong Zhou,† Yaping Huang,† Hengrui Yang,† Dujin Wang,*,† and Duanfu Xu†

State Key Laboratory of Polymer Physics and Chemistry, Institute of Chemistry, The Chinese Academy of Sciences, Beijing 100080, China, and Key Laboratory for Colloid and Interface Chemistry of Education Ministry, School of Chemistry and Chemical Engineering, Shandong University, Ji'nan 250100, China

Received: September 8, 2005; In Final Form: December 23, 2005

The fast mixing of aqueous solutions of calcium chloride and sodium carbonate could immediately result in amorphous calcium carbonate (ACC). Under vigorous stirring, the formed ACC in the precipitation system will dissolve first and, then, transform within minutes to produce crystalline forms of vaterite and calcite. After that, the solution-mediated mechanism dominates the transformation of the thermodynamically unstable vaterite into the thermodynamically stable calcite. Although ACC is the least stable form of the six anhydrous phases of calcium carbonate ($CaCO_3$), it could be, however, produced and stabilized by a variety of organisms. To better understand the formation−transformation mechanism of ACC and vaterite into calcite, ex-situ methods (i.e., scanning electron microscopy, Fourier transform infrared spectroscopy, and X-ray diffraction spectroscopy) were used to characterize the formation−transformation process of ACC and vaterite in aqueous systems without organic additives, showing that ACC sampled at different conditions has different properties (i.e., lifetime, morphology, and spectrum characterization). It is also very interesting to capture the obviously polycrystalline particles of $CaCO_3$ during the transformation process from vaterite to calcite, which suggests the formation mechanism for the calcite superstructure with multidimensional morphology.

1. Introduction

Biological materials have unique structures and morphologies, which acquire much better performance than the relatively crude minerals.[1,2] More than 60 kinds of inorganic minerals have been found in various organisms, the most common one of which is calcium carbonate.[3] In organisms, calcium carbonate has polymorphs of calcite, aragonite, and to a lesser extent vaterite and monohydrate. The amorphous form is the least stable phase of calcium carbonate, which is supposed to be used as reservoirs of $CaCO_3$ ions during the animal molting period.[4] These have aroused great interest in people to investigate the crystallization and growth mechanism of $CaCO_3$ and to prepare $CaCO_3$ with specific form, size, morphology, and structure for more than 100 years.[5] One of the facile ways for $CaCO_3$ preparation is to mix the aqueous solutions of calcium chloride and sodium carbonate, which partly modulates the unwanted scale-forming minerals in heat exchangers and in crude oil production.[6−8] In this fast-reactive crystallization process, the calcium ions and carbonate groups combine into the amorphous $CaCO_3$, the most instable solid-state phase. Then, the initially formed amorphous calcium carbonate (ACC) transforms within a few minutes to a mixture of several crystalline $CaCO_3$. The transformed carbonates are vaterite and calcite at low temperatures (14−30 °C) and aragonite and calcite at high temperatures (60−80 °C). At intermediate temperatures (40−50 °C) the transformed phase contains all of the three varieties.[9] The stability of the $CaCO_3$ solids decreases in the following order: ACC < vaterite < aragonite < calcite. Actually, the stability and lifetime of these polymorphic species mainly depend on the properties of additives and their own solubilities in aqueous solution.[9−11]

In one of our past works,[12] much attention was paid to the transformation process of vaterite to calcite, confirming that this transformation in aqueous solution at ambient conditions took place through dissolution of vaterite and followed by the crystallization of calcite.[13,14] Up until now, it is also very difficult to directly observe the dissolution and transformation process of vaterite; furthermore, it is almost impossible to view in situ the dissolution process of the ACC phase.[15,16] Of course, the dissolution and transformation processes of metastable anhydrous $CaCO_3$, obtained in the spontaneous precipitation systems, can be detected in the presence of organic additives and/or magnesium ions.[17,18] Although the modern technologies, such as X-ray microscopy and the small-angle X-ray scattering,[15,19] are more suitable for characterizing in situ the formation and growth of $CaCO_3$ particles in aqueous systems, they are not the intuitionistic way to observe the obtained particles. Actually, the classically ex-situ methods, such as scanning electron microscopy (SEM) picture, can partly satisfy the solid-phase conversions and the recrystallization phenomena during the $CaCO_3$ precipitation process. In this paper, the formation−dissolution process of amorphous calcium carbonate at different pH values was investigated by means of SEM and Fourier transform infrared (FT IR) methods. Among these experimental results, the obviously polycrystalline particles of $CaCO_3$ during the transformation process from vaterite to calcite were captured. This can be used to explain the formation mechanism of the calcite superstructure with multidimensional morphology.

2. Experimental Section

$CaCl_2$ and Na_2CO_3 were of analytical grade and were used without further purification. Doubly deionized water was used

* Corresponding authors. E-mail: qshen@sdu.edu.cn (Q.S.); djwang@iccas.ac.cn (D.W.).
† The Chinese Academy of Sciences.
‡ Shandong University.

10.1021/jp055063o CCC: $33.50
Published on Web 01/27/2006

to prepare aqueous $CaCl_2$ and Na_2CO_3 solutions just before each experiment. Solution pH was measured by a combination of electrodes (Mettler Toledo HA405-K2/120, ±0.01 pH), calibrated before and after each experiment by the two standard buffer solutions of tartrate (25 °C, pH = 3.56) and borate (25 °C, pH = 9.18).

Calcium carbonate was precipitated by rapidly pouring aqueous $CaCl_2$ solution into a 300 mL beaker containing an equal volume of Na_2CO_3 solution. During the precipitation process, the reactant solution was continuously stirred at a constant rate of 200 rpm by means of a Telflon-coated magnetic stirring bar, keeping the homogeneity of the ion concentration and of the pH value. The total volume of the working solution was 200 mL, and the initially different supersaturation solutions were employed to investigate the formation and transformation mechanisms of amorphous $CaCO_3$ and vaterite in the spontaneous precipitation process of $CaCO_3$. The initial concentration of aqueous $CaCl_2$ (or Na_2CO_3) solution was selected at 50 and 100 mM, respectively, and all experiments were conducted at 26 ± 0.2 °C in a thermostatic bath.

The pH value of 50 or 100 mM $CaCl_2$ solution has the same value of 6.35, while the pH values of 50 and 100 mM Na_2CO_3 solutions are 11.58 and 11.71, respectively. So, the initial concentration of $CaCl_2$ or Na_2CO_3 solution not only affected the initial supersaturation degree of $CaCO_3$ but also had effect on the initial pH of the reactant system. Before mixing the aqueous solutions of 50 mM $CaCl_2$ and 50 mM Na_2CO_3, the pH value of the Na_2CO_3 solution was adjusted to pH 12.0 by the addition of 0.10 M NaOH solution. The pH value of the precipitation systems changed with time, due to the variation of the CO_3^{2-} concentration, which was tracked by immersing a pH electrode in the reaction beaker. At each interval, the precipitated solids were immediately collected by filtering through cellulose nitrated/acetate membrane filters (0.2 μm), and directly laid on the KBr matrix and immediately used for IR measurement. This way was the best for detecting the existence of amorphous $CaCO_3$ with a lifetime of several minutes;[9] of course, it could also overcome the effect of the KBr-grinding method on crystal forms. For SEM measurements, the filtered $CaCO_3$ was predried in a vacuous desiccator cabinet at 26 °C for at least 24 h.

All samples were Au-coated prior to examination by a Hitachi S-4300 scanning electron microscope, fitted with a field emission source and operating at an accelerating voltage of 15 kV. The Fourier transform infrared spectra were recorded by a Bruker IFS 100 FT-Raman spectrometer with 4 cm^{-1} divergence. The X-ray diffraction (XRD) patterns were collected on a Rigaku D/max-2400 powder X-ray diffractometer with Cu Kα radiation (40 kV, 120 mA). The 0.02° steps/(25 s) and the 2θ range from 20 to 60° were selected to analyze the crystal structure and orientation.

3. Results and Discussion

3.1. Formation−Dissolution Process of ACC. At the beginning of the experiments Ca^{2+} and CO_3^{2-} ions combine into amorphous calcium carbonate, which is the most unstable form and is often described in spherical shapes of diameter lower than 1 μm, in the temperature range between 10 and 55 °C.[9] To understand the formation of ACC and its transformation in solution with time, precipitation experiments were performed at various time intervals. And then, the collected precipitates were ex-characterized by using SEM, XRD, and FT IR methods, which could be partly used to in-situ investigate the morphological changes and phase transformation of ACC. Figure 1 shows pictures of the $CaCO_3$ spheres, with average 600 nm (400−800 nm) in diameter, obtained at 10 s after the rapidly mixing of $CaCl_2$ and Na_2CO_3. The lack of any sharp peaks in the XRD pattern for this precipitate confirmed the formation of the ACC spheres (Figure 2e). According to Cho's results, the ACC film shows a split peak at 1472 and 1384 cm^{-1} (ν_3), the broad ν_2 absorption of the carbonate out-of-plane bending peak at 866 cm^{-1}, and the symmetric stretch adsorption at 1070 cm^{-1} (ν_1), respectively, and the ν_3 and ν_1 adsorption peaks will concurrently shift to the relatively high wavenumber, respectively.[17] However, the FT IR spectrum (Figure 2a) of these spherical samples (Figure 1) shows adsorption peaks at 1082, 876, and 712 cm^{-1} and indicates the existence of a calcite phase.[18] Only the split peak at 1418 and 1339 cm^{-1}, resembling that of ACC (ν_3) at 1472 and 1384 cm^{-1},[17] might be assigned to the characteristic adsorption of ACC. Herein, the ACC was prepared by rapidly mixing the aqueous solutions of 100.0 mM $CaCl_2$ and 100.0 mM Na_2CO_3, while that in ref 17 was prepared from 20 mM $CaCl_2$ solution by the diffusion of ammonium carbonate. Is it due to the high $CaCl_2$ concentration (or, the low pH value of the precipitation solution) that makes the shift of ν_3? Even if it is right, the reason the ν_1 adsorption of the ACC phase did not shift concurrently is mysterious.

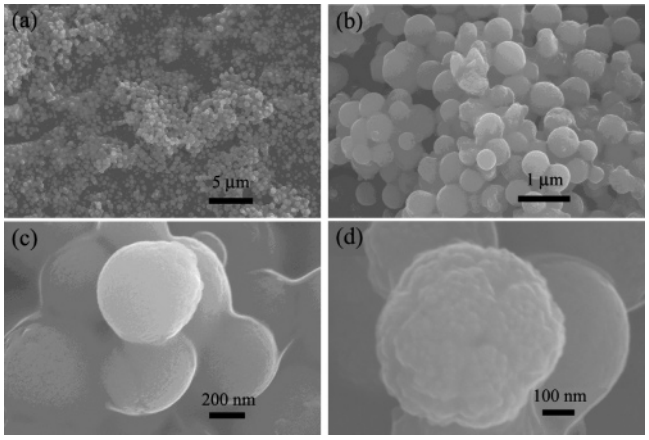

Figure 1. SEM images of the precipitated $CaCO_3$ particles sampled at 10 s after the rapid mixing of equal volumes of 100.0 mM $CaCl_2$ and 100.0 mM Na_2CO_3 solutions. Panels a−d are the gradually magnified picture.

Around 10 s the pH value of the precipitation system is decreasing, and the unstable pH value means the existence of dissociative ions because of the high supersaturation degree of the Ca^{2+}(aq) or CO_3^{2-}(aq) ions. It is supposed that, even at a continuous stirring rate of 200 rpm, the formation of ACC continues during the following process of filtering and drying, resulting in the gelatiniform $CaCO_3$ to connect spherical ACC particles (Figure 1b,c). Generally, the lifetime of ACC is too short to distinguish the time period between its formation and transformation. However, the transformation of ACC into crystalline $CaCO_3$ could cause the release of water from ACC.[20−22] If the drying and the exposition under electron beam could release water from ACC spheres, the rough surfaces of these ACC spheres shown in Figure 1d are probably due to the transformation of ACC to crystalline forms. The FT IR spectra of $CaCO_3$ obtained at 5 and 10 s after the rapid mixing of the reactants (aqueous solutions of 100.0 mM $CaCl_2$ and 100.0 mM Na_2CO_3) are illustrated in Figure 2a,b, respectively. Although no rhombohedral calcite was directly observed in the SEM pictures (Figure 1), the peaks at 712 and 876 cm^{-1} (Figure 2a,b) assigned to the ν_4 and ν_3 absorption bands of calcite, respectively, confirm the phase transformation of ACC to calcite.[18,23]

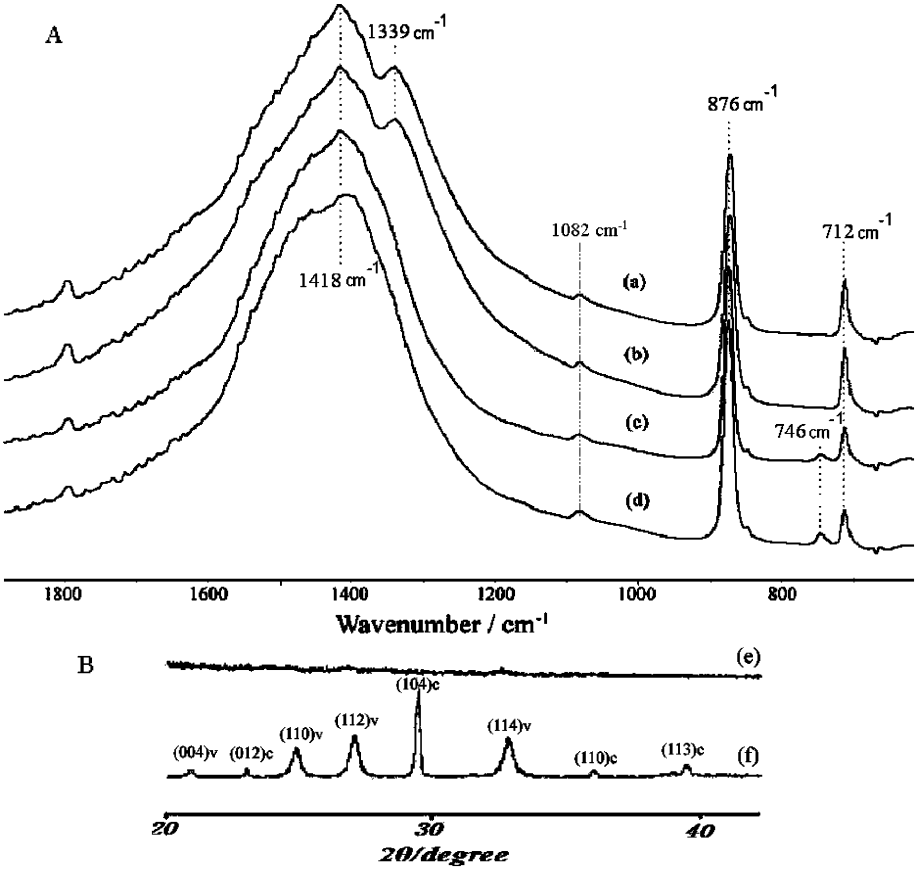

Figure 2. FT IR (A) and XRD (B) spectra of the $CaCO_3$ precipitates sampled at various intervals after the rapid mixing of 100.0 mM reactant solutions: (a) 5, (b and e) 10, (c) 30, and (d and f) 60 s.

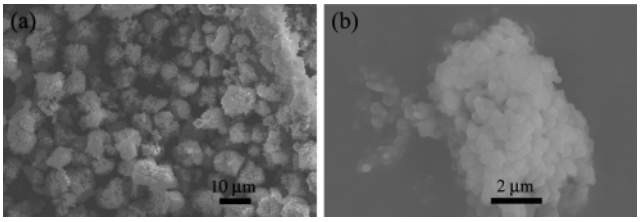

Figure 3. SEM images of the precipitated $CaCO_3$ particles sampled 30 s after the rapid mixing of equal volumes of 100.0 mM reactant solutions. Panel b is the magnified picture of a.

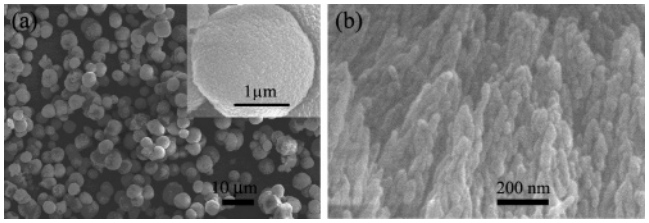

Figure 4. (a) SEM image of the precipitated $CaCO_3$ particles sampled at 60 s after the rapid mixing of equal volumes of 100.0 mM reactant solutions. The inset is the SEM picture of a spherical vaterite. (b) SEM image showing the rough morphology of a spherical surface.

Parts c and d of Figure 2 show the FT IR spectra of $CaCO_3$ sampled at 30 and 60 s after the rapid mixing of reactants, respectively. The $CaCO_3$ particles obtained at 30 s are shown in Figure 3a, and the magnified picture of which clearly shows the heterogeneous and rough property of the particle surface (Figure 3b). The comparison of Figure 3 with Figure 1d suggests that a much greater amount of ACC solids obtained from the precipitation solution at this interval should be transferred into crystalline forms.[20−22] It is well-known that in the $CaCO_3$ precipitation system the initially formed ACC will transform to the two crystalline phases of vaterite and calcite.[7,12] So, the appearance of the characteristic peak of vaterite (745 cm^{-1}) and the ν_4 and ν_3 absorption bands of calcite (Figure 2c,d) indicate that the transformation of ACC takes place in the precipitation system. The coexistence of vaterite and calcite can also be proved by the XRD results shown in Figure 2f.[12] In other words, the formation of polycrystalline particles of $CaCO_3$ took place at ca. 30 s after the mixing of reactants. The dissolution of ACC resulted in rough surfaces of ACC particles, suggesting the solution-mediated mechanism for ACC transformation.

It can also be seen that parts c and d of Figure 2 show one broad absorption peak at 1418 cm^{-1} and the different peak-intensity ratio of I_{746}/I_{712}. According to Andreassen's opinion, even at the high stirring of 1500 rpm, the ACC will transform within several minutes to produce the major spherical and crystalline vaterite.[7] So, the disappearance of the split peak in the FT IR spectrum does not mean the complete transformation of ACC in bulk phase. The relatively higher ratio of I_{746}/I_{712} at 60 s (Figure 2d) than that at 30 s (Figure 2c) indicates that at 60 s the transformed polycrystalline solid contains the relatively higher percentage of vaterite. This can also be proved by the SEM images for the precipitated $CaCO_3$ shown in Figure 4. The SEM picture of Figure 4a and its magnified inset clearly show the spherical morphology of polycrystalline solids. The high-resolution image (Figure 4b) shows the amorphous nature of the spherical surface, which can be used to interpret the aggregation and/or growth behavior of vaterite particles.[7,12]

It is well-known that various conditions (i.e., the solution composition, temperature, pH, stirring, mixing rate of reactants, and supersaturation level, etc.) affect the crystallization habit

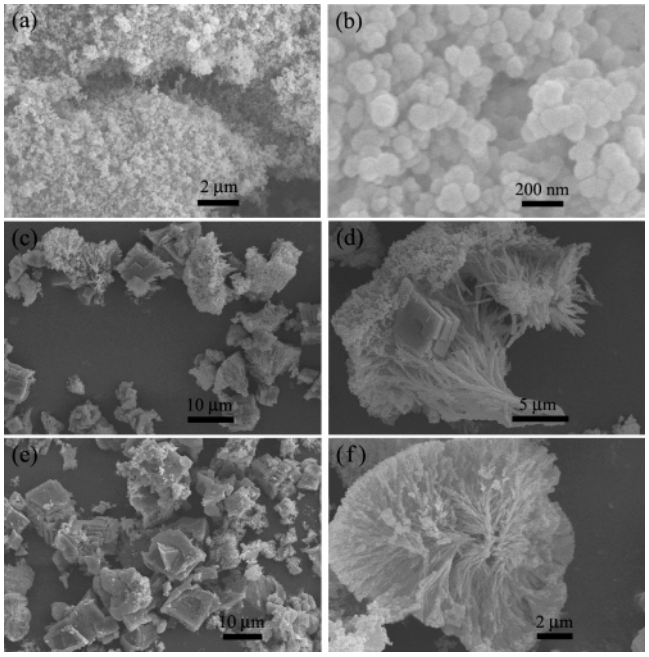

Figure 5. SEM images of the precipitated $CaCO_3$ particles sampled at various intervals after the rapid mixing of equal volumes of 50.0 mM $CaCl_2$ and 50.0 mM Na_2CO_3 solutions. The pH value of Na_2CO_3 solution was adjusted to 12.0 before mixing. Panels a and b represent the morphology of the $CaCO_3$ obtained at 5 s; c and d, 30 s; and e and f, 60 s.

of $CaCO_3$. According to Andreassen's opinion, the supersaturation value is fixed at a level determined by the dissolution of ACC during the transformation.[7] To clarify these observations listed above, $CaCO_3$ precipitation was conducted again at a completely different condition (i.e., a relatively lower reactant concentration and a relatively higher pH value than before). Before mixing, both of the reactant concentrations were cut down to 50 mM, and the pH value of Na_2CO_3 solution was adjusted to 12.0. The formation−dissolution process of ACC was also tracked by SEM, XRD, and FT IR methods. Herein, the XRD patterns (data not shown) show almost the same results as these shown in Figure 2B, for example, the coexistence of vaterite and calcite and the increase of the peak-intensity ratio of I_{746}/I_{712} with time, etc. Although the XRD results indicate the same phase transformation mechanism of ACC, the SEM pictures and FT IR spectra are quite different from those listed before. Parts a and b of Figure 5 show the formation of spherical ACC at 5 s after the rapid mixing of equal volume of 50.0 mM reactant solutions, the amorphous nature of these spheres can be proved by FT IR measurements (Figure 6a). Figure 6a shows a split peak at 1481 and 1414 cm^{-1}, the absorption band at 1073 cm^{-1}, and the broad absorption band at 864 cm^{-1}, and these peaks can precisely be assigned to the ν_3, ν_2, and ν_1 characteristics of ACC, respectively.[17,18] The ν_3 adsorption of ACC (at 1472 and 1384 cm^{-1}) in ref 17 is different from that at 1481 and 1414 cm^{-1} in Figure 6a, together with the split peak at 1418 and 1339 cm^{-1} shown in Figure 2A, which might prove the uncertain property of the symmetric adsorption of carbonate group.

The $CaCO_3$ precipitates sampled at 10 and 30 s show the same IR spectral characteristics of ACC, which are illustrated in Figure 6b,c, respectively. All of these FT IR spectra (i.e., Figure 6a−c) show a broad absorption band at 713 cm^{-1}, indicating the coexistence of the crystalline phase of calcite. The appearance of rhombohedral $CaCO_3$ particles in SEM pictures (Figure 5c,d) supports the above anticipation for the transformation mechanism of ACC induced by evaporation of water.[20,22] When the initial supersaturation level is relatively low, the resulted ACC particles acquire the relatively low quantity and small size. Then, the continuous formation of ACC at this supersaturation level causes the aggregation behavior of ACC particles in an irregular manner (Figure 5d). Even at 60 s after the rapid mixing of reactant solutions (50.0 mM), the obtained samples only show the dried flakes of ACC (Figure 5e), and the dissolution of ACC and the transformed polycrystalline particles of vaterite and calcite were not detected by SEM observation (Figure 5f) and FT IR characterization (Figure 6d), respectively. However, the sharpening absorption band at 713

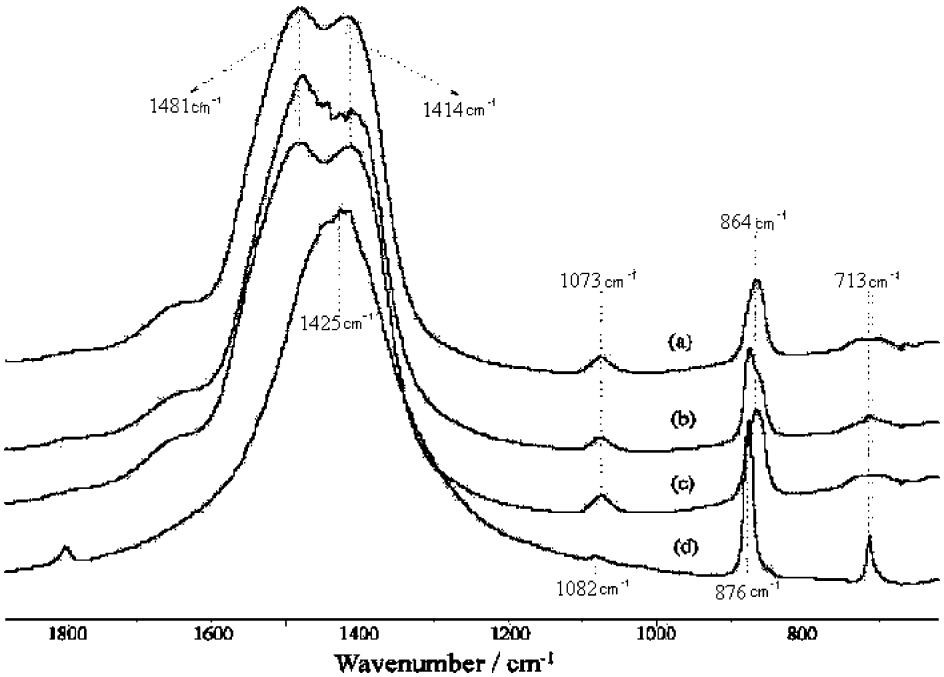

Figure 6. FT IR spectra of the $CaCO_3$ precipitates sampled at different incubation times of 5 (a), 10 (b), 30 (b), and 60 s (d), respectively, after the rapid mixing of 50.0 mM reactant solutions.

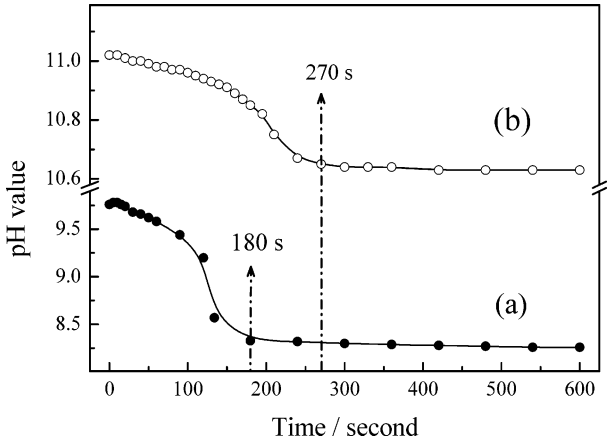

Figure 7. Variation of pH value with incubation time at different conditions: solid circles (a), the directly mixing of 100 mM reactant solutions; open circles (b), the pH value of Na_2CO_3 solution adjusted to 12.0 before directly mixing of 50 mM reactant solutions. Arrows represent the lifetime of ACC.

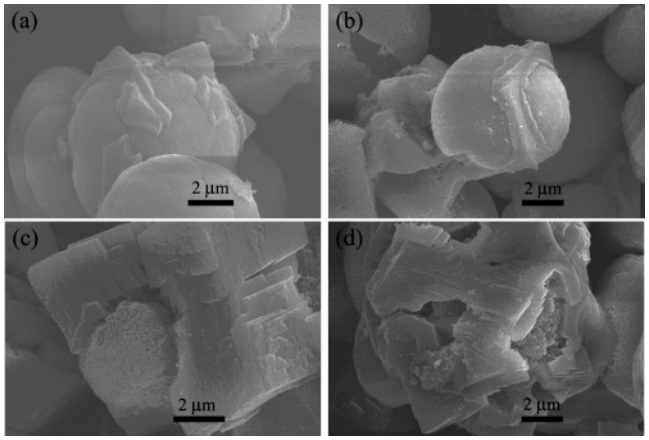

Figure 8. SEM images of the polycrystalline $CaCO_3$ particles sampled at various intervals after the rapidly mixing of equal volumes of 100.0 mM reactant solutions: (a) 10, (b and c) 30, and (d) 60 min.

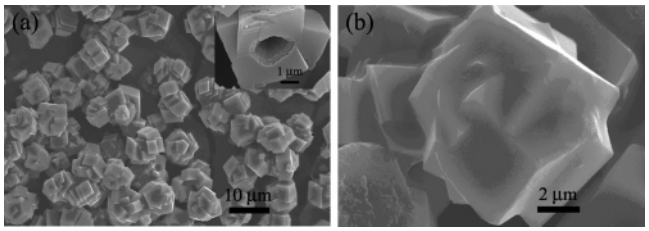

Figure 9. (a) SEM images of the precipitated $CaCO_3$ particles sampled at 4 h after the rapid mixing of equal volumes of 100.0 mM reactant solutions. The inset in it shows a calcite superstructure with a hole on {104} faces. Panel b is the magnified picture of a typical calcite particle selected from a.

cm^{-1} and the change of the double-peak band to a broad band at 1425 cm^{-1}, as well as the ca. 10 cm^{-1} "blue shift" of the ν_1 and ν_2 absorption bands of ACC, suggest that the dissolution of ACC particles starts after 30 s incubation.

Here, we would like to cite a similar report on the characterization of ACC by means of differential scanning calorimetry:[24] the collected ACC solids experienced two exothermic processes at 105 and 149 °C, corresponding to the transformation of ACC to a crystalline product and the evaporation of water, respectively. According to Wegner's hypothesis—the formation of amorphous $CaCO_3$ is subjected to liquid−liquid-phase segregation[24]—water contained in the "dried" amorphous $CaCO_3$ could also induce the formation of crystalline forms. This suggests that ex-situ methods cannot be used to determine the lifetime of ACC.

It should be mentioned that the synthesized $Ca(OH)_2$ solids only show the typical spectral characteristic at 3640 cm^{-1}.[25] This implies that the initial pH value of Na_2CO_3 at 12.0 has almost no influence on the FT IR adsorption of ACC appearing in the range from 600 to 1700 cm^{-1}. Another interesting phenomenon should also be pointed out that the pH value of $CaCO_3$ precipitation systems changes with incubation time. After rapidly mixing the aqueous solutions of 100.0 mM $CaCl_2$ (pH = 6.35) and 100.0 mM Na_2CO_3 (pH = 11.71), the pH of the precipitation systems changes from 9.76 at first ($t \sim 0$ s) to 8.26 at 600 s. Similarly, after rapidly mixing the aqueous solutions of 50.0 mM $CaCl_2$ (pH = 6.35) and 50.0 mM Na_2CO_3 (pH = 12.00), the pH of the precipitation systems changes from 11.01 ($t \sim 0$ s) to 10.63 ($t \sim 600$ s). In fact, when the initial pH of the 50.0 mM Na_2CO_3 solution (pH = 11.58) was adjusted to a value of 12.0, a lower amount of 0.10 M NaOH solution was added. This means that the adjustment of the pH value of the initial 50.0 mM Na_2CO_3 solution has nearly no influence on the ionic strength of the precipitation system. So, despite the initial supersaturation level, the initial pH value was also believed to play an important role in the phase transition of $CaCO_3$ solids. The experimental results of the in-situ pH measurements are shown in Figure 7.

At the different experimental conditions the pH value of the precipitation systems decreased slowly at first; then, it experienced a sharp decrease to reach a plateau within 5 min. It has been mentioned by Andreassen[7] that this sharp decrease of pH value indicates the complete dissolution of ACC. After the direct mixing of 100 mM reactant solutions, the resulting ACC has a lifetime of 180 s (Figure 7a). When the pH value of the initial 50 mM Na_2CO_3 solution was adjusted to 12.0 before mixing, the addition of an equal volume of 50 mM $CaCl_2$ resulted in the ACC with a longer lifetime of 270 s (shown in Figure 7b). So, it is concluded that the resulting ACC at different conditions has different lifetimes. It is supposed that the solution-mediated mechanism of ACC transformation could partly be prohibited during the drying stage, and, the in-situ pH measurement also confirms to some extent the SEM, FT IR, and XRD results on the formation−dissolution mechanism of ACC.

3.2. Formation of Calcite Superstructure. After the dissolution of ACC the transformed crystalline forms are the kinetically stable vaterite and thermodynamically stable calcite under the experimental condition.[9] Then, the solution-mediated mechanism dominates the transformation of spherical vaterite to rhombohedral calcite.[12] It is very difficult to estimate whether the dissolution of vaterite or the crystallization step of calcite is the rate-controlling process. However, it is very interesting to capture the obviously polycrystalline particles of $CaCO_3$ during the transformation process from vaterite to calcite (Figure 8). These polycrystalline particles from Figure 8a to Figure 8d were obtained at different times during the transformation process of vaterite, all of which indicate the heterogeneous nucleation mechanism of calcite on the spherical surface of vaterite. [30]

When these polycrystalline particles (Figure 8) were kept in the precipitation system for a long period of time, the dissolution of vaterite continued. In the meantime, the crystallization and growth of calcite on the surface of polycrystalline spheres resulted in various calcite superstructures (Figure 9a). One of the typical calcite superstructures is presented in Figure 9b, showing the multidimensional morphology. The inset in Figure 9a shows a calcite superstructure with a hole on {104} faces.

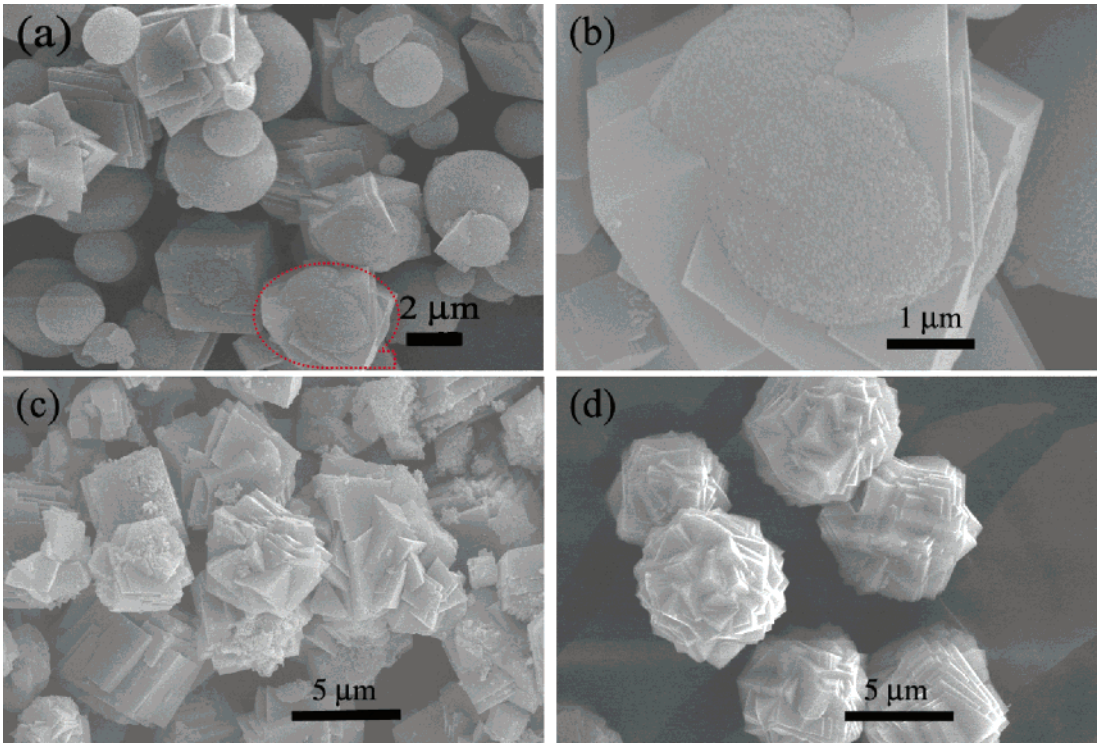

Figure 10. SEM images of the precipitated $CaCO_3$ particles sampled at various intervals after the rapid mixing of equal volumes of 50.0 mM reactant solutions: (a and b) 10, (c) 30, and (d) 60 min, respectively. The pH value of Na_2CO_3 solution was adjusted to 12.0 before mixing. Panel b is the magnified picture of a polycrystalline particle marked in a.

In controlling the crystallization process of $CaCO_3$, various organic templates have been used to synthesize inorganic superstructures. When mineralization occurs on the surface of organic templates, the size and shape of templates, even the chemical structure and concentration of organic additives, control the form of the mineralized materials.[26−29] Herein, the unstable phase of $CaCO_3$ solid (i.e., the spherical vaterite) could also be used as a "soft" template to generate calcite with a hole on {104} faces (Figure 8c and the inset in Figure 9a). And, this supports the nucleation and growth mechanism of the calcite superstructure with multidimensional morphology.

When the initial pH value of 50 mM Na_2CO_3 solution (pH = 11.58) was adjusted to 12.0 before mixing, the addition of an equal volume of 50 mM $CaCl_2$ into the reaction beaker was also used to test the formation mechanism of the calcite superstructure. After the complete dissolution of ACC, the transformed mixture of vaterite and calcite was anticipated. At an incubation time of 10 min the obtained specimens are shown in Figure 10a. In this SEM picture (Figure 10a), a polycrystalline particle during the transformation process from vaterite to calcite was marked, the morphology of which was also magnified and presented in Figure 10b. Although the transformation of vaterite would continue for about 8 h,[12] the grown calcite superstructures with multidimensional morphology were observed at an interval of 30 (Figure 10c) and 60 min (Figure 10d), respectively. The observation of a polycrystalline particle (Figure 10b) and the calcite superstructure (Figure 10d) in an intuitionistic manner further supports the mentioned hypothesis for the template action of spherical vaterite.

4. Conclusion

The unstable forms of $CaCO_3$ (i.e., ACC) can be stabilized and investigated more precisely, due to the operation in a complex system and the improvement of experimental techniques, respectively. Especially in recent years, the amorphous calcium carbonate has further become the hottest topic because it is a precursor in the formation of more stable crystalline forms. Although the lifetime of ACC is only several minutes in "pure water", the ex-situ methods can also be used to observe its formation, to characterize its properties, and to conclude its solution-mediated transformation mechanism. In our previous works, the calcite particle with a hole on {104} faces and the calcite superstructure with multidimensional morphology were always observed, the formation mechanism of which is another purpose in this presentation. If the surface of a spherical vaterite provides several active sites for the heterogeneous nucleation of calcite crystals, the continuous dissolution of vaterite and the growth of each calcite nuclei result in these calcite superstructures.

Acknowledgment. The financial support from the National Natural Science Foundation of China (Grant 20471064) and the Natural Science Found of Shandong Province (Grant Y2004B05) is gratefully acknowledged.

References and Notes

(1) Currey, J. D. *J. Zool. (1965−1984)* **1979**, *188*, 301−308.
(2) Currey, J. D. In *The Mechanical Properties of Biological Materials*; Vincent, J. F. V., Currey, J. D., Eds.; Cambridge University Press: Cambridge, U.K., 1980; pp 75−97.
(3) Currey, J. D.; Kohn, A. J. *J. Mater. Sci.* **1976**, *11*, 1615−1623.
(4) Raz, S.; Testeniere, O.; Hecker, A.; Weiner, S.; Luquet, G. *Biol. Bull. (Beijing)* **2002**, *203*, 269−274.
(5) Nancollas, G. H.; Reddy, M. M. *J. Colloid Interface Sci.* **1971**, *37*, 824−830.
(6) Shen, Q.; Wei, H.; Zhao, Y.; Wang, D. J.; Zheng, L. Q.; Xu, D. F. *Colloids Surf., A.* **2004**, *251*, 87−91.
(7) Andreassen, J.-P. *J. Cryst. Growth* **2005**, *274*, 256−264.
(8) Dawe, R. A.; Zhang, Y. P. *J. Pet. Sci. Eng.* **1997**, *18*, 179−187.
(9) Elfil, H.; Roques, H. *Desalination* **2001**, *137*, 177−186.
(10) Cechova, M.; Alince, B.; van de Ven, T. G. M. *Colloids Surf., A* **1998**, *141*, 153−160.
(11) Tsuno, H.; Kagi, H.; Akagi, T. *Bull. Chem. Soc. Jpn.* **2001**, *74*, 479−486.

(12) Wei, H.; Shen, Q.; Zhao, Y.; Wang, D.-J.; Xu, D.-F. *J. Cryst. Growth* **2003**, *250*, 516−524.
(13) Katsifaras, A.; Spanos, N. *J. Cryst. Growth* **1999**, *204*, 183−190.
(14) Manoli, F.; Dalas, E. *J. Cryst. Growth* **2000**, *218*, 359−364.
(15) Rieger, J.; Thieme, J.; Schmidt, C. *Langmuir* **2000**, *16*, 8300−8305.
(16) Pontoni, D.; Bolze, J.; Dingenouts, N.; Narayanan, T.; Ballauff, M. *J. Phys. Chem. B* **2003**, *107*, 5123−5125.
(17) Xu, X. R.; Han, J. T.; Cho, K. *Chem. Mater.* **2004**, *16*, 1740−1746.
(18) Ajikumar, P. K.; Wong, L. G.; Subramanyam, G.; Lakshminarayanan, R.; Valiyaveettil, S. *Cryst. Growth Des.* **2005**, *5*, 1129−1139.
(19) Bolze, J.; Peng, B.; Dingenouts, N.; Panine, P.; Narayanan, T.; Ballauff, M. *Langmuir* **2002**, *18*, 8364−8369.
(20) Raz, S.; Weiner, S.; Addadi, L. *Adv. Mater.* **2000**, *12*, 38−42.
(21) Xu, X. R.; Han, J. T.; Cho, K. *Langmuir* **2005**, *21*, 4801−4804.
(22) Aizenberg, J.; Muller, D. A.; Grazul, J. L.; Hamann, D. R. *Science* **2003**, *299*, 1205−1208.
(23) Aizenberg, J.; Lambert, G.; Weiner, S.; Addadi, L. *J. Am. Chem. Soc.* **2002**, *124*, 32−39.
(24) Faatz, M.; Gröhn, F.; Wegner G. *Adv. Mater.* **2004**, *16*, 996−1000.
(25) The standard FT IR spectrum for the synthesized calcium hydroxide powder in the manipulation software of the Nicolet Magna-750 IR spectrometer.
(26) Mann, S.; Ozin, G. A. *Nature* **1996**, *382*, 313−318.
(27) Walsh, D.; Lebeau, B.; Mann, S. *Adv. Mater.* **1999**, *11*, 324−328.
(28) Liang, P.; Shen, Q.; Zhao, Y.; Zhou, Y.; Wei, H.; Lieberwirth, I.; Huang, Y. P.; Wang, D. J.; Xu, D. F. *Langmuir* **2004**, *20*, 10444−10448.
(29) Rudloff, J.; Cölfen, H. *Langmuir* **2004**, *20*, 991−996.
(30) Liu, X. Y. *J. Chem. Phys.* **2000**, *112*, 9949−9955.